4-1-2011

Soil Carbon and Material Fluxes Across the Eroding Alaska Beaufort Sea Coastline

Chien-Lu Ping
University of Alaska Fairbanks, cping@alaska.edu

Gary J. Michaelson
University of Alaska Fairbanks, gjmichaelson@alaska.edu

Laodong Guo
University of Southern Mississippi, guol@uwm.edu

M. Torre Jorgensen
ABR, Inc., ecoscience@alaska.net

Mikhail Z. Kanevskiy
University of Alaska Fairbanks, mkanevskiy@alaska.edu

See next page for additional authors

Soil carbon and material fluxes across the eroding Alaska Beaufort Sea coastline

Chien-Lu Ping,[1] Gary J. Michaelson,[1] Laodong Guo,[2] M. Torre Jorgenson,[3] Mikhail Kanevskiy,[4] Yuri Shur,[4] Fugen Dou,[5] and Jingjing Liang[6]

Received 22 October 2010; revised 7 January 2011; accepted 26 January 2011; published 20 April 2011.

[1] Carbon, nitrogen, and material fluxes were quantified at 48 sampling locations along the 1957 km coastline of the Beaufort Sea, Alaska. Landform characteristics, soil stratigraphy, cryogenic features, and ice contents were determined for each site. Erosion rates for the sites were quantified using satellite images and aerial photos, and the rates averaged across the coastline increased from 0.6 m yr^{-1} during circa 1950–1980 to 1.2 m yr^{-1} during circa 1980–2000. Soils were highly cryoturbated, and organic carbon (OC) stores ranged from 13 to 162 kg OC m^{-2} in banks above sea level and averaged 63 kg OC m^{-2} over the entire coastline. Long-term (1950–2000) annual lateral fluxes due to erosion were estimated at −153 Gg OC, −7762 Mg total nitrogen, −2106 Tg solids, and −2762 Tg water. Total land area loss along the Alaska Beaufort Sea coastline was estimated at 203 ha yr^{-1}. We found coastal erosion rates, bank heights, soil properties, and material stores and fluxes to be extremely variable among sampling sites. In comparing two classification systems used to classifying coastline types from an oceanographic, coastal morphology perspective and geomorphic units from a terrestrial, soils perspective, we found both systems were effective at differentiating significant differences among classes for most material stores, but the coastline classification did not find significant differences in erosion rates because it lacked differentiation of soil texture.

Citation: Ping, C.-L., G. J. Michaelson, L. Guo, M. T. Jorgenson, M. Kanevskiy, Y. Shur, F. Dou, and J. Liang (2011), Soil carbon and material fluxes across the eroding Alaska Beaufort Sea coastline, *J. Geophys. Res.*, *116*, G02004, doi:10.1029/2010JG001588.

1. Introduction

[2] Coastal erosion and release of organic carbon (OC) to nearshore waters of the Beaufort Sea, Alaska depends on numerous terrestrial and oceanographic factors, including exposure to open ocean and fetch length, nearshore bathymetry, and onshore factors, such as topography, bank height, soil properties, and ground ice. The properties are extremely heterogeneous along the coastline and have been poorly quantified. *Hartwell* [1973] differentiated the coastline of northern Alaska as mostly fronted by barriers islands (34%) or eroding shoreline (37.5%), while deltaic accretion represents nearly 20% of the total coastline. *Jorgenson and Brown* [2005] refined the coastal classification on the basis of the compilation of previous studies and interpretation of Landsat imagery. They differentiated five basic coastal types along the 1957 km Alaskan Beaufort Sea coast: exposed bluffs (313 km), bays and inlets (235 km), lagoons with barrier islands (547 km), tapped basins (thaw lake basins) (171 km) and deltas (691 km) (Figure 1). Bank heights generally are low (2–4 m), especially for deltas [*Jorgenson and Brown*, 2005]. Surficial deposits along the coast are typically fine-grained fluvial, eolian, lacustrine, and marine deposits, and thus bedrock control is lacking [*Wahrhaftig*, 1965; *Black*, 1964; *Dinter et al.*, 1990]. Ground ice contributes to erosion rates because it affects slope movement and formation of wave-cut niches that destabilize ice-rich bluffs [*Leffingwell*, 1919; *Harper*, 1978; *Walker*, 1983; *Dallimore et al.*, 1996]. Although extremely variable, the variation in ice contents is strongly linked to geomorphic processes [*Shur and Jorgenson*, 1998; *Pullman et al.*, 2007]. Of particular importance is the abundance of ice wedges, which is strongly associated with geomorphic processes and range in volume from 1 to 30% (M. Kanevskiy et al., Ground ice in the upper permafrost of the Alaskan Beaufort Sea coast, submitted to Antarctic, Arctic, and Alpine Research, 2011).

[1]Palmer Research Center, School of Natural Resources and Agricultural Sciences, University of Alaska Fairbanks, Palmer, Alaska, USA.
[2]Department of Marine Science, University of Southern Mississippi, Stennis Space Center, Mississippi, USA.
[3]ABR Inc., Fairbanks, Alaska, USA.
[4]Department of Civil and Environmental Engineering, University of Alaska Fairbanks, Fairbanks, Alaska, USA.
[5]Texas AgriLife Research and Extension Center, Texas A&M University, Beaumont, Texas, USA.
[6]Department of Forest Sciences, School of Natural Resources and Agricultural Sciences, University of Alaska Fairbanks, Fairbanks, Alaska, USA.

0148-0227/11/2010JG001588

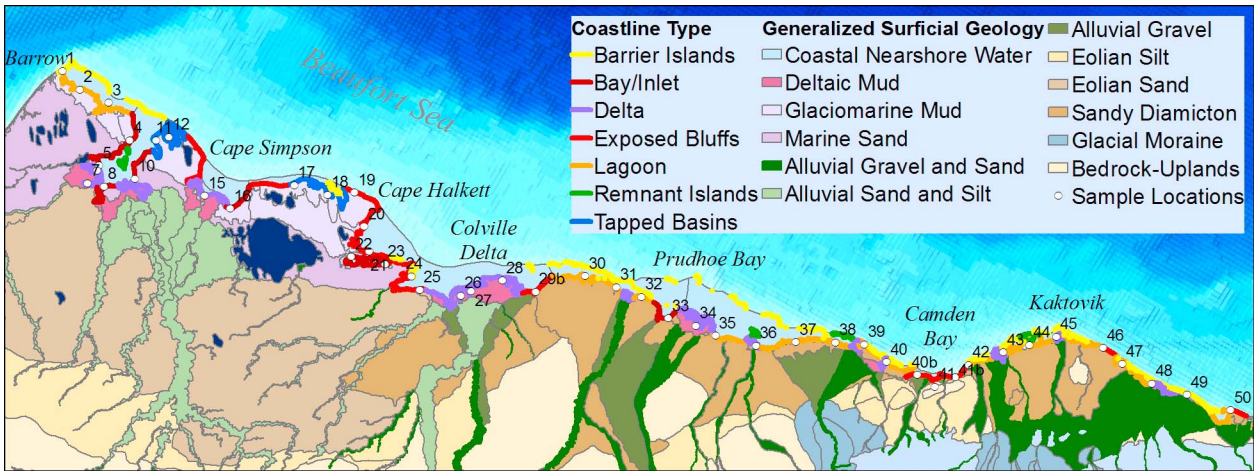

Figure 1. General coastline types and generalized surficial geology along the Beaufort Sea coast, northern Alaska.

[3] Large quantities of OC stored in permafrost and the Arctic carbon cycle plays an important role in both atmospheric and marine processes [*Gilmanov and Oechel*, 1995; *Michaelson et al.*, 1996; *Stein and Macdonald*, 2004; *Davidson and Janssens*, 2006; *Ping et al.*, 2008]. If climatic changes continue, a larger portion of OC currently sequestered in northern ecosystems would likely be remobilized and transported to aquatic systems [*Guo et al.*, 2007; *McGuire et al.*, 2009]. A hypothesized climate-driven increase in terrestrial OC inputs to the Arctic Ocean through permafrost thawing, accelerated coastal erosion, and increasing river runoff could dramatically change the turnover and transport rates of tundra carbon, and alter biogeochemical cycles and the arctic ecosystem [*Gibson et al.*, 2000; *Savelieva et al.*, 2000; *Stein and Macdonald*, 2004; *McGuire et al.*, 2009]. Of particular interest is the rapid release of soil OC that has been sequestered in permafrost for thousands of years. Much of this OC accumulated during 5–9 ka ago and the OC is commonly found to depths of 2–3 m in older coastal plain deposits [*Ping et al.*, 1997; *Jorgenson and Brown*, 2005]. Major lateral OC export from land to the Arctic Ocean includes fluxes from coastal erosion and river discharge. Recent studies have estimated OC fluxes through large Arctic rivers to the Arctic Ocean [e.g., *Raymond et al.* 2007; *Guo et al.*, 2011]. However, few studies have quantified the total soil organic carbon flux from coastal erosion to the Arctic [*Jorgenson and Brown*, 2005; *McGuire et al.*, 2009]. To better quantify these fluxes, the Arctic Coastal Dynamics program [*Brown and Solomon*, 2000] initiated a major circumpolar effort to compile existing data and estimate coastal erosion rates and OC fluxes into the Arctic Ocean. In an initial assessment of the Alaskan Beaufort Sea section, *Jorgenson and Brown* [2005] estimated that eroding shorelines across the 1957 km coast of the Beaufort Sea contributes 1.8×10^5 Mg OC yr^{-1}, but this study was a first-order estimation and highlighted the fact that most parameters were inadequately quantified using soils data from only five previously studied sites and confidence limits could not be assigned to the estimates.

[4] Accordingly, the goal of this project was to better quantify OC inputs in order to help evaluate the importance of the transformation of carbon and other substances in the dynamic coastal zone as a critical process that links coastal erosion to the C biogeochemical cycles in the Arctic Ocean. Specific objectives were to: (1) quantify the carbon, nitrogen, soil material stores, and ice contents at systematically distributed sites; (2) to relate these stores to the physical environments along the coast; and (3) to estimate total fluxes of these elements across the Alaskan Beaufort Sea coast (ABSC). In assessing carbon fluxes, we quantified stores and fluxes in relation to two common classification systems, a coastline classification that emphasizes shoreline exposure and bank morphology from an oceanographic perspective and a geomorphic classification that emphasizes soil materials and terrain evolution from a terrestrial perspective.

2. Materials and Methods

[5] A total of 48 extensive study sites were systematically selected at 40 km intervals along the 1957 km of the ABSC (see Figure 1 and Table 1). A systematic design was used in order to reduce sampling bias, broadly distribute samples across the entire coast, and because no geomorphic maps exist at large enough scale and accuracy to allow a stratified random design. Once at the predetermined locations, the actual sampling location along the bluff was situated at the nearest bank to the extent possible. Soil sampling was done between ice wedges, for which relative volume was estimated separately. Samples were obtained from undisturbed permafrost after removal of refrozen slump material. A vertical face along the coastal bank was cleaned back into the unthawed soil profile. The width of the exposed face ranged from 1 to 3 m to cover the cyclic patterns of the cryoturbated soil profile. Soil cores (50–200 cm^3) were taken from the exposed soil horizons down to sea level using electric hand drills with keyhole coring saw blades. At low flat sites lacking bluffs, soil pits were excavated and soil cores were taken to the depth of seasonal thawing; then a 7.5 cm diameter SIPRE core was used to drill and obtain frozen cores to sea level, usually up to 2 m depth. At each site, geomorphic characteristics, permafrost-related microtopographic features, shoreline morphology, vegetation, and soil stratigraphy were recorded. Geomorphic units were classified according to engineering geology terminology

Table 1. Characteristics of 48 Sampling Locations Along the Beaufort Sea Coast, Alaska[a]

						Erosion Rate (m yr^{-1})			TOC Flux	Ice Wedge	Bank Height Stores (kg m^{-2})							
Site	Latitude (°N)	Longitude (°W)	Coastal Type[b]	Geomorphic Unit[c]	Bank Height (m)	1950–2000	1950–1980	1980–2000	1950–2000 (kg yr^{-1})	Volume (%)	H_2O	Solids	TOC	TN	Ca	Mg	K	Na
1	71.337	156.593	LG	IPB	0.4	−0.55	−0.64	−0.31	−16	3	294	457	29	1.6	1.22	0.42	0.14	1.12
2	71.259	156.336	LG	IRB	2.3	−1.66	−1.76	−1.56	−136	22	1785	757	82	4.3	2.40	0.59	0.08	0.09
3	71.212	155.926	LG	IRB	1.4	−5.19	−3.76	−4.57	−410	8	1151	422	79	4.3	1.61	0.46	0.04	0.13
4	71.048	155.592	BI	SDM	1.6	−2.65	−2.47	−2.25	−164	12	1254	755	62	3.1	2.12	0.44	0.05	0.33
5	70.919	155.980	DT	IRB	0.4	−0.66	−0.65	−0.82	−22	5	300	157	34	1.7	0.41	0.12	0.01	0.12
6	70.895	155.997	DT	ES	2.5	−0.48	−0.35	−0.59	−18	10	642	3365	36	0.5	8.16	0.49	0.07	0.27
7	70.834	156.111	DT	DTA	0.5	−0.02	−0.01	−0.19	<1	8	316	593	18	0.7	1.70	0.39	0.02	0.02
8	70.825	155.883	BI	DTA	1.2	−0.83	−0.24	−1.50	−35	15	862	547	42	2.4	2.55	0.29	0.02	0.08
10	70.874	155.485	BI	SDM	4.0	−0.97	−0.66	−1.32	−119	13	2614	2472	122	6.9	13.30	1.31	0.21	0.73
11	71.057	155.240	TB	IRB	2.3	−2.72	−1.29	−3.81	−220	4	2018	567	81	4.5	2.74	0.46	0.06	0.07
12	71.076	155.068	TB	IRB	1.4	−0.92	−0.26	−1.79	−56	10	1026	598	62	3.3	2.03	0.49	0.09	0.27
15	70.820	154.532	DT	DTA	0.4	−1.35	−0.44	−2.14	−40	10	344	233	30	1.5	0.97	0.32	0.06	0.78
16	70.768	154.177	BI	IRB	3.1	−1.59	−1.62	−1.07	−217	9	2262	1165	137	7.9	7.88	1.00	0.32	0.37
17	70.893	153.338	TB	IPB	0.5	−2.75	−2.05	−3.47	−53	1	208	467	19	1.3	1.11	0.47	0.17	0.70
18	70.856	152.882	TB	IRB	0.9	−0.19	0.03	−0.73	−5	5	637	313	24	1.3	1.00	0.30	0.06	0.28
19	70.871	152.522	EB	GLM	2.6	−8.52	−3.10	−13.31	−848	12	1698	1052	100	5.3	1.29	0.39	0.04	0.17
20	70.716	152.382	EB	IRB	2.5	−1.56	−0.45	−2.70	−165	2	1836	1344	106	5.8	0.53	0.15	0.02	0.13
21	70.602	152.298	EB	SDM	3.0	−2.12	−2.00	−2.31	−129	4	2355	1706	61	2.5	10.65	0.87	0.10	0.49
22	70.576	152.538	BI	SDM	4.5	−0.69	−0.88	−0.05	−87	6	3680	1889	127	6.7	11.45	0.96	0.14	1.19
23	70.547	152.088	BI	IRB	3.0	−0.56	−0.25	−0.92	−60	6	2380	961	107	5.5	5.37	0.93	0.06	0.59
24	70.496	151.733	EB	ES	3.2	−0.29	−0.25	−0.24	−25	8	551	4631	86	3.1	27.41	0.65	0.10	0.40
25	70.435	151.617	EB	ES	3.0	0.12	0.06	0.15	9	10	1090	3703	75	2.4	22.82	0.92	0.14	0.28
26	70.411	151.073	DT	IPB	1.2	0.22	0.48	−0.62	6	3	742	809	29	1.2	1.78	0.73	0.26	1.33
27	70.433	150.939	DT	DTA	1.6	−0.48	−0.14	−0.85	−32	8	1192	711	67	3.6	2.60	0.72	0.10	1.16
28	70.483	150.531	DT	DTA	0.6	−1.18	−0.89	−1.22	−15	0	349	663	13	0.7	0.96	0.56	0.18	0.74
29b	70.433	150.094	EB	SDM	2.8	−0.98	−0.79	−1.11	−159	11	2073	986	162	9.4	12.75	0.77	0.03	0.81
30	70.504	149.439	LG	SDM	2.0	−0.99	−0.14	−2.00	−82	8	709	2733	83	1.0	22.66	0.39	0.07	0.18
31	70.450	149.026	LG	IRB	2.0	−0.58	−1.17	1.55	−21	10	771	1997	37	1.7	14.71	0.25	0.02	0.14
32	70.405	148.701	LG	SDM	2.6	−0.97	−0.75	−1.24	−78	12	1418	1725	80	1.8	12.74	0.57	0.03	0.36
34	70.267	147.994	DT	ES	3.0	−0.43	−0.26	−0.33	−64	3	1420	3029	149	1.4	23.83	0.23	0.02	0.05
35	70.218	147.744	LG	IRB	0.4	−1.59	−1.39	−1.92	−44	10	259	324	28	1.6	1.31	0.34	0.02	0.49
36	70.165	147.221	DT	IRB	1.4	−1.78	−0.29	−0.34	−102	17	1014	254	57	3.7	1.08	0.23	0.01	0.08
37	70.173	146.703	LG	OGD	0.2	−0.16	−0.13	−0.91	−2	5	194	84	14	1.0	0.41	0.27	0.06	1.11
38	70.162	146.183	LG	SDM	1.4	0.01	−0.16	0.46	<1	12	916	583	81	3.3	5.43	0.32	0.01	0.09
39	70.145	145.810	LG	SDM	2.5	−0.78	−1.16	−0.35	−62	10	1744	1642	79	3.7	10.07	0.77	0.06	0.23
40	70.057	145.535	LG	SDM	2.8	−0.12	−0.08	−0.12	−14	10	1847	1493	114	6.1	14.77	0.68	0.03	0.05
40b	69.989	145.151	EB	OGD	3.5	−0.35	−1.29	1.11	−36	15	2326	1940	103	4.0	14.63	1.32	0.09	0.82
41	69.930	144.939	EB	EL	3.4	-	-	-	-	50	2012	1072	39	1.7	8.69	0.77	0.06	0.16
41b	69.964	144.672	EB	EL	4.0	−0.15	−0.02	−0.36	−10	50	1794	1482	66	3.3	10.86	0.81	0.08	0.08
42	70.016	144.483	LG	OGD	2.0	−0.14	0.00	−0.26	−6	15	582	1611	43	2.7	2.25	0.57	0.04	0.08
43	70.061	144.019	DT	ES	1.7	−0.01	0.12	0.24	<1	0	430	2328	20	0.9	7.12	0.27	0.01	0.04
44	70.082	143.671	LG	DTA	0.3	-	-	-	-	6	249	153	24	1.5	0.59	0.26	0.04	0.59
45	70.108	143.315	DT	ES	2.5	−0.21	−0.38	0.02	−8	0	653	3474	39	1.1	19.51	0.43	0.02	0.13
46	70.036	142.723	LG	SDM	3.0	−1.05	−1.40	−0.54	−119	11	1890	1665	114	6.0	17.08	1.66	0.13	1.57
47	69.952	142.505	LG	SDM	3.2	−0.33	0.91	−0.96	−24	15	2230	2127	74	2.1	18.13	0.96	0.08	0.26
48	69.849	142.157	DT	DTA	1.0	−0.31	0.57	−0.77	−10	4	525	879	30	1.3	5.43	0.47	0.06	0.54
49	69.777	141.724	DT	DTA	0.4	−0.06	−0.03	0.02	−1	0	176	498	13	0.2	4.59	0.06	0.01	0.08
50	69.683	141.196	EB	SDM	3.5	−2.06	−0.74	−3.88	−259	16	1926	2319	126	5.9	19.47	1.10	0.17	0.17

[a]Stores and fluxes are adjusted for ice wedge volume estimates.
[b]Coastal types are as follows: BI, bay/inlet; DT, delta; EB, exposed bluff; LG, lagoon; TB, tapped basin.
[c]Geomorphic units are as follows: DTA, delta and tidal flat; EL, eolian loess; ES, eolian sand; GLM, glaciomarine; IPB, ice-poor basin; IRB, ice-rich basin; OGD, other gravel deposits; SDM, sandy diamicton.

developed for Alaska [*Kreig and Reger*, 1982]. Ground ice structure and permafrost geomorphic features were described on the basis of the work of *Shur and Jorgenson* [1998]. Ice wedge cross-sectional dimensions were measured at each site. Ice wedge polygon size was estimated for each site using aerial or satellite photography. Ice wedge volumes at each site were calculated with wedge shape assumed to be triangular and prism shaped to allow volume to be calculated for the permafrost layers (Kanevskiy et al., submitted manuscript, 2011).

[6] Soil samples were obtained at 20 cm depth increments, although slight adjustments were sometimes made to avoid sampling across soil horizon breaks. The cores were measured for volume in the field, sealed in plastic bags, and transferred to the laboratory where they were weighed and air-dried. Subsamples were dried to 105°C and reweighed for moisture content. Samples with gravel were sieved (2 mm sieve) to determine the weight of coarse fragments prior to chemical analysis of the fine fraction. Total carbon (TC) and nitrogen (TN) were determined on dried samples using a LECO CHN analyzer at the UAF-AFES Palmer Plant and

Soil Analysis Laboratory. Samples with pH of 5.5 or greater were acid treated and C evolved as CO_2 was determined and subtracted from the amount of TC to give total organic carbon (TOC). Extractable K, Ca, Mg and Na were determined by ICP spectroscopy on neutral 1 N ammonium acetate extracts of air-dried samples [*Soil Survey Laboratory Staff*, 1996].

[7] For each site dry matter (weight of solids), water content, TOC, and TN storage from the surface down to sea level were calculated using the equation of *Michaelson et al.* [1996]. For example:

$$\text{OC storage}\left(\text{kg m}^{-2}\right) = \text{T} * \text{D}_\text{b} * (\%\,\text{OC}) \cdot 10^{-1} * \left(1 - \left(\%\,\text{CF}_\text{v} \cdot 10^{-2}\right)\right) * \left(1 - \left(\%\,\text{SIW}_\text{v} \cdot 10^{-2}\right)\right),$$

where T is horizon thickness (cm), D_b is bulk density (g cm^{-3}), CF_v is volumetric percentage of rock fragments >2 mm in diameter, and SIW_v is the site ice wedge volume percentage. Standard deviations and confidence intervals were from above calculated data using Excel spreadsheet functions. The stores in individual soil horizons above sea level were summed as recommended by the ACD protocols [*Brown and Solomon*, 2000] for calculating coastal erosion fluxes. Total soil mass for each profile was calculated from bulk density and horizon depth measurements. Water storage of each site was similarly calculated from sample weight loss after drying (Table 1).

[8] Erosion rates along the ABSC were measured from ~1950 (1949–1955) black and white air photos, ~1980 (1978–1982) CIR air photos, and ~2000 (2000–2004) imagery that included Quickbird satellite images from Elson Lagoon and the Arctic National Wildlife Refuge, a controlled CIR air photo mosaic for the National Petroleum Reserve Alaska, and a true color controlled mosaic for the central ABSC. The historical air photos were scanned at 1200 dpi and georectified to the ~2000 imagery using distinct features evident on the imagery. RMS errors generally were less than 3 m. After georectification, 1 km of coastline across the sampling location was delineated using ArcGIS for each of the three periods at the 48 extensive sites along the coast. We defined the coastline as the water's edge because it allowed us to map coastlines over the range of vegetated and nonvegetated geomorphic units and the tidal range (20 cm) is small. The Digital Shoreline Analysis Systems [*Thieler et al.*, 2005], an extension for ArcGIS, was used to divide the coastline into 10 segments and calculate the distance between the three coastlines for each endpoint of the segments. We calculated a mean erosion rate from the 10 measurements for each sampling site for the ~1950 to ~1980, ~1980 to ~2000, and ~1950 to ~2000 periods (Table 1).

[9] Shorelines at the 48 sites were classified using two systems to help partition the variability of properties and fluxes of highly heterogeneous soil materials and coastal morphologies (Table 1). We used the coastal classification system as described by the Arctic Coastal Dynamics program [*Brown and Solomon*, 2000; *Jorgenson and Brown*, 2005] to be consistent with the circumpolar effort to estimate carbon fluxes into the Arctic Ocean. This allows our data to be extrapolated across broader regions using the ACD database. The geomorphic classification, which was modified slightly from the terrain unit classification of *Kreig and Reger* [1982] is designed to differentiate surficial processes. This system helps differentiate surface ages and ground ice characteristics associated with a typical surface microtopography. The geomorphic system allows extrapolation of soil properties across the broader coastal plain on the basis of properties of similar units. One-way analysis of variance (ANOVA) was used to test the effects of coastal type and geomorphic unit on soil properties.

3. Results

3.1. Coastline Characteristics

[10] The ABSC was classified into five coastline types: exposed bluff, bay/inlet, lagoon-barrier islands, tapped basins, and deltas (Table 1). Delta deposits (35% of the coastline length), were most abundant along the entire coast at the mouths of numerous rivers. Lagoon barrier island systems (28%) were second most common along the entire coast and were frequently associated with sandy diamicton deposits, which provide a good source of sand and gravel for the barrier islands. Exposed bluffs (16% of coast) were abundant from Cape Halkett to Cape Simpson (Figure 1). These bluffs lack the protection by barrier islands and storm fetch in late summer can be hundreds of kilometers. Large bays or inlets (12%) occurred mostly in the western portion of the study area. Tapped basins (9%) were abundant in the same area because lakes and drained basins were common in the glaciomarine deposits in this area.

3.2. Geomorphic Units

[11] On the basis of interpretation of soil structures and texture, the 48 sites were classified into 8 geomorphic units including: sandy diamicton of glacial origin, glaciomarine, other gravelly deposits (old beach ridge, alluvial fan, braided floodplain), eolian sand (active and inactive), eolian loess, ice-rich drained lake basins (centers and margins), ice-poor drained lake basins (centers and margins), delta-tidal flats (abandoned and inactive delta floodplain, and active and inactive tidal flats; see Table 1 and Figure 1).

[12] Sandy diamicton was the most abundant deposit along the coast (27% of sites). It had a wide particle-size distribution and was often gravelly, high in segregated ice and moderately high in wedge ice content (Figure 2). The deposit was slightly saline even though it occurred up to 60 km inland, and generally lacked plant and animal fossils at depth. It has recently been attributed to an ice sheet from the continental shelf [*Jorgenson and Shur*, 2008] and is of Late Pleistocene age. The height of bluffs at most sites varied from 2 to 4 m and the land surface usually had well developed high center polygons. Nearly all the sites had 20% frost boils and well developed surface organic horizons around them. The active layer was <1 m and all sites had a reduced mineral matrix within the surface 50 cm.

[13] Ice-rich drained lake basins (25% of sites) were low-lying areas surrounded by large areas of the older raised surfaces. The basins were formed through thawing of the ice-rich permafrost within the older raised surfaces. Also, some of these basins were formed simply as depressions within an undulating sand sheet [*Jorgenson et al.*, 2006]. Drained basins were commonly found within the older glaciomarine and sandy diamicton deposits and are features

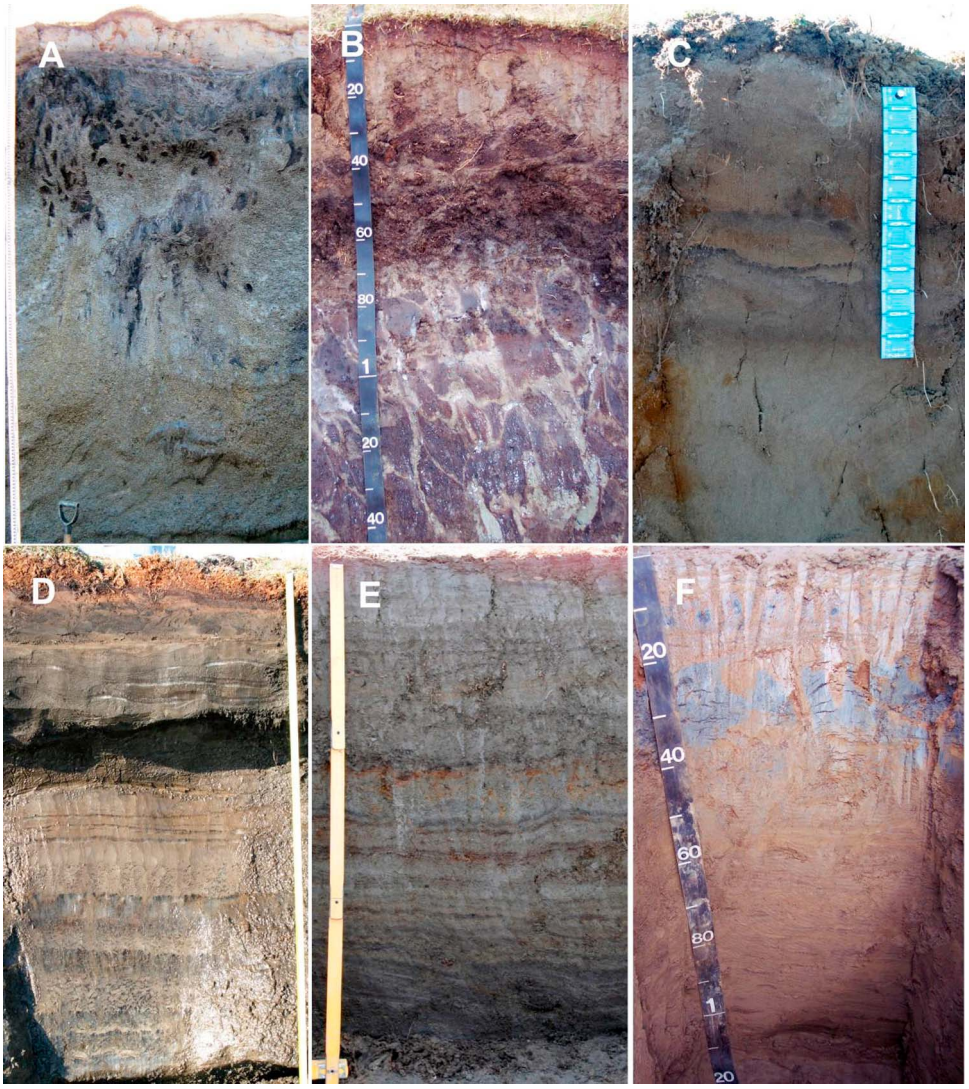

Figure 2. Photographs of soil profiles of dominant geomorphic units, including (a) glaciomarine, (b) sandy diamicton, (c) inactive eolian, (d) ice-rich drained basin, (e) ice-poor drained basin, and (f) tidal flat deposits.

of early to mid-Holocene age. Ice-rich basins had abundant low-center polygons. The soils were loamy to sandy and often slightly gravelly, with high contents of segregated and wedge ice (Figure 2).

[14] Delta and tidal flat deposits (17% of sites) were abundant along the entire coastline and had fine-grained stratified soils. Delta deposits include inactive floodplains with moderately thick interbedded organic and mineral horizons, whereas delta abandoned floodplains occurred further from the coast and had thick accumulations of peat. Tidal flats were barren owing to frequent addition of new sediment. Outer portion of most deltas lacked well-developed polygons with only the early stages of cryoturbation present owing to the continued addition of sediments. Segregated ice, however, was abundant near the top of the permafrost.

[15] Eolian sand (13% of sites) was abundant and associated with both active dunes on deltas and with inactive dunes within a large Late Pleistocene sand sea [*Carter*, 1981]. The material and the soils formed in it lacked gravel, had low silt and clay content, and had little segregated and wedge ice. The surface morphology varied from flat- to high-centered polygons. Cryoturbation was weak in the sandy soils, and only noticed at half of the sites as distorted horizons and involutions below the permafrost table.

[16] Glaciomarine deposits (2% of sites) were restricted to the Cape Halkett and Cape Simpson areas, where they relatively high bluffs (4–7 m) and were frequently exposed to the open ocean. They were composed of slightly pebbly silty clay loam (Figure 2), had abundant marine fossils and occasional cobbles, and were extremely ice rich. The land surface commonly had both flat- and high-centered polygons. There was a dense concentration of organic matter near the permafrost table and to a depth of more than 150 cm, forming a very distinct pattern caused by the dark brown or black organic contrasting with the bluish gray mineral glaciomarine deposits. These soils had 8 to 11 cm of surface organic horizon, and organic matter accounted for 20–30% by volume of the upper 50 cm. Although we sample only one site, we maintained it as a separate class because of its unusually high ice contents and erosion rates.

[17] Other gravelly deposits (6% of sites) of differing geomorphic origins were combined into a group of uncommon disparate types with single occurrences for analysis purposes. Most of these sites were located on older Pleistocene age portions of the landscape, and tended to be gravelly with high segregated ice contents but low wedge ice contents (Figure 2). The group included an old beach ridge with stratified sands and gravels, an abandoned floodplain with alluvial gravels below the fine-grained cover material, and abandoned cover deposit on a braided floodplain with channel gravels at depth.

[18] Ice-poor drained lake basins (6% of sites) of relative young age had poorly developed ice wedges and lack of visible (prominent) ice wedge polygonal patterns. While uncommon, we included them because of their distinct characteristics associated with tapped lakes. They were more common along coastlines with tapped basins, particularly near Cape Simpson and Cape Halkett, 80 km east of Barrow. The soils had only thin surface peat layers and lacked cryoturbation.

[19] Eolian loess (4% of sites) was restricted to high bluffs along Camden Bay. Soils were composed mostly of silt, and had high segregated and wedge ice contents. The surface was characterized with large high-centered polygons with the exception of site 41b, which was characterized by large conical thermokarst, mounds and large thermoerosional gullies along the high bluffs. Cryoturbation was prevalent. Although ice-rich silt is highly erodable, the part of coast with these deposits was fronted by a wide gravel beach that protected the loess bluff from wave action. Gravel on the beach was delivered presumably by along shore currents from nearby braided gravelly floodplains.

3.3. Carbon, Mineral, and Water Stores

[20] Stores of materials for each site were calculated on the basis of the bank height above sea level measured at each site and presented on a 1 m^2 surface area basis (Table 1). The material stores were adjusted for volumes of ice wedges and they include organic carbon (OC), total nitrogen (N), total solids (soils), water, and selected major cations such as Na, K, Ca, and Mg. The average carbon and other material stores within both coastline types and geomorphic units for the banks above sea level are presented in Table 2.

[21] There were significant variations (ANOVA, $P < 0.05$) in most sites and soil properties among coastal types and geomorphic units (Table 3). For coastal types, 6 of 12 properties varied significantly. Notable exceptions were the recent and long-term erosion rates presumably because variability was so high with classes. For geomorphic units, 11 of 12 properties varied significantly, with most being highly significant ($P = 0.00$) and K being the sole exception. The results indicate that the geomorphic units were overall more effective at partitioning the variability in site and soil properties than were coastal types, as evident by the substantially lower P values for soil and site properties associated with the geomorphic units.

[22] For coastal types, carbon and material stores typically varied twofold to fourfold among classes (see Table 2 and Figure 3). Mean OC stores were highest for exposed bluffs and bay/inlets (92–99 kg m^{-2}), intermediate for lagoons (64 kg m^{-2}), and lowest in tapped basins (46 kg m^{-2}) and deltas (41 kg m^{-2}). Average total N stores were highest for bay/inlets and exposed bluffs (5.4–4.3 kg m^{-2}), intermediate for lagoons and tapped basins (2.8–2.6 kg m^{-2}), and lowest for deltas (1.4 kg m^{-2}). Mean solids content (dry weight of mineral plus organics) was highest for exposed bluffs (2023 kg m^{-2}), intermediate for deltas and bay/inlets (1307–1298 kg m^{-2}), and lowest for lagoons and tapped basins (1185–486 kg m^{-2}). Mean water content was highest for bay/inlets (2175 kg m^{-2}) and exposed bluffs (1766 kg m^{-2}), intermediate for lagoons and tapped basins (1069–972 kg m^{-2}), and lowest for deltas (623 kg m^{-2}). Mean bank height was highest for exposed bluffs (3.2 m) and bay inlets (2.9 m), intermediate for lagoons (1.8 m), and lowest for deltas (1.3 m) and tapped basins (1.3 m). In general, soil material stores increased with increasing bank heights across sites. For example, TOC was strongly related ($R^2 = 0.50$) to bank height (Figure 4). However, the strength of these relationships varied across properties with R^2 for solids, H_2O, TN, Ca, Mg, and Na being 0.45, 0.65, 0.30, 0.45, 0.46, and 0.34, respectively.

[23] For geomorphic units, bank stores typically varied four to over sixfold among classes (see Table 2 and Figure 3). Mean bank OC stores were highest in glaciomarine, sandy diamicton, and loess deposits (100–99 kg OC m^{-2}), intermediate in ice-rich basins, eolian sand, and other gravelly (69–53 kg OC m^{-2}), lowest in delta-tidal flat deposits and ice-poor drained lake basins (30–26 kg OC m^{-2}). Mean bank total N stores were highest for glaciomarine deposits (5.3 kg m^{-2}), intermediate for sandy diamicton, ice-rich drained lake basins, other gravelly deposits, and eolian loess, (4.5–2.5 kg m^{-2}), and lowest for eolian sand, delta-tidal flats and ice-poor drained lake basins (1.6–1.4 kg m^{-2}). Mean bank solids content was highest for eolian sand and sandy diamicton (3422–1700 kg m^{-2}), intermediate for eolian loess, other gravelly deposits, and glaciomarine (1277–1052 kg m^{-2}), and lowest for ice-rich drained lake basins, ice-poor drained lake basins, and deltas (738–519 kg m^{-2}). Mean bank water content was highest for eolian loess, sandy diamicton, glaciomarine deposits, ice-rich drained lake basins, and other gravelly deposits (1903–1043 kg m^{-2}), intermediate for eolian sand (798 kg m^{-2}), and lowest for deltas, and ice-poor drained lake basins (483–415 kg m^{-2}). Mean bank height was highest for eolian loess, sandy diamicton, eolian sand, and glaciomarine deposits (3.7–2.6 m), intermediate for other gravelly deposits and ice-rich drained lake basins (1.9–1.8 m), and lowest for deltas, and ice-poor basins (0.8–0.7 m).

3.4. Mean Annual Material Fluxes

[24] Annual flux of soil materials into the Beaufort Sea is a function of erosion rates, bank heights and material stores. Site OC fluxes based on the long-term 1950–2000 erosion rates are given in Table 1 and the average estimated fluxes for OC by coastal type and geomorphic unit groups are given in Table 2. The overall coastline weighted average flux rate, taking into account coastal types composition across the study area, was -73 ± 36 kg m^{-1} yr^{-1} TOC (Table 2). The overall coastline fluxes (solids, water, carbon, nitrogen and major elements) are presented in Table 4.

[25] Using erosion rates for the long-term period (1950–2000), early period (1950–1980), and recent period (1980–

Table 2. Unit Average Soil Carbon, Nitrogen, and Material Stores for Coastal Types and Geomorphic Units and Coastline Total Organic Carbon Flux According to Coastal Types and Geomorphic Units[a]

	Erosion Rate 1950–2000 (m yr^{-1})	Bank Height (m)	Total Stores in Bank (kg m^{-2})								Coastline Average TOC Flux (kg m^{-1} yr^{-1})
			Solids	Water	TOC	TN	K	Ca	Mg	Na	
Coastal Type											
Delta											
average (N = 13)	−0.5	1.3	1307	623	41	1.4	0.06	6.01	0.39	0.41	−21
SD	0.6	0.9	1255	379	36	1.1	0.08	7.43	0.21	0.46	19
Lagoon											
average (N = 15)	−1.0	1.8	1185	1069	64	2.8	0.06	8.36	0.57	0.43	−64
SD	1.3	1.0	829	702	32	1.7	0.04	7.70	0.37	0.47	32
Exposed bluff											
average (N = 10)	−1.8	3.2	2023	1766	92	4.3	0.08	12.91	0.78	0.35	−163
SD	2.7	0.5	1225	556	35	2.3	0.05	8.63	0.33	0.27	62
Bay/inlet											
average (N = 6)	−1.2	2.9	1298	2175	99	5.4	0.13	7.11	0.82	0.55	−121
SD	0.8	1.3	737	1008	39	2.2	0.12	4.61	0.38	0.39	47
Tapped basin											
average (N = 4)	−1.6	1.3	486	972	46	2.6	0.09	1.72	0.43	0.33	−76
SD	1.3	0.8	129	773	30	1.6	0.05	0.82	0.09	0.27	49
Coastal average[b]											
average (N = 48)	**−1.0**	**1.9**	**1315**	**1148**	**63**	**2.9**	**0.08**	**7.53**	**0.56**	**0.42**	**−73**
CI (P = 0.05)	±0.7	±0.6	±561	±390	±21	±1.0	±0.04	±3.88	±0.17	±0.24	±36
Geomorphic Unit											
Sandy diamicton											
average (N = 13)	−1.1	2.8	1700	1897	99	4.5	0.08	13.12	0.83	0.50	−100
SD	0.8	0.9	643	769	31	2.5	0.06	5.58	0.38	0.46	71
Ice-rich basin											
average (N = 12)	−1.6	1.8	738	1287	69	3.8	0.06	3.42	0.44	0.23	−122
SD	1.3	0.9	544	745	36	2.0	0.08	4.17	0.28	0.17	118
Ice-poor basin											
average (N = 3)	−1.0	0.7	577	415	26	1.4	0.19	1.37	0.54	1.05	−21
SD	1.5	0.4	200	287	6	0.2	0.06	0.36	0.17	0.32	30
Delta											
average (N = 8)	−0.6	0.8	519	483	30	1.5	0.06	2.42	0.38	0.50	−19
SD	0.5	0.5	218	334	18	1.1	0.06	1.77	0.20	0.41	11
Eolian sand											
average (N = 6)	−0.2	2.7	3422	798	67	1.6	0.06	18.14	0.50	0.19	−18
SD	0.2	0.5	761	378	47	1.0	0.05	8.52	0.26	0.14	26
Eolian loess											
average (N = 2)	−0.2	3.7	1277	1903	53	2.5	0.07	9.77	0.79	0.12	−10
SD	-	0.4	290	154	19	1.2	0.01	1.53	0.03	0.06	-
Glaciomarine											
average (N = 1)	−8.5	2.6	1052	1698	100	5.3	0.04	1.29	0.39	0.17	−848
SD	-	-	-	-	-	-	-	-	-	-	-
Older gravel deposits											
average (N = 3)	−0.2	1.9	1212	1034	53	2.6	0.06	5.76	0.72	0.67	−15
SD	0.1	1.7	990	1136	45	1.5	0.03	7.73	0.54	0.53	19

[a]Determined on the basis of the 1950–2000 average erosion rates and coastline coastal type segment lengths. All stores and fluxes include adjustments for ice wedge volume. Abbreviations are as follows: CI, 95% confidence interval; SD, standard deviation; TN, total nitrogen; TOC, total organic carbon. Bold values are the averages weighted by costal type occurrence.
[b]Weighted by lengths of the coastal types.

2000), the mean annual flux of OC from coastal erosion along the 1957 km coastline was estimated at −153 ± 24, −98 ± 15, and −178 ± 28 Gg TOC yr^{-1}, respectively (Table 4). The large 95% confidence intervals of the estimates were due to the high variability of the estimates for unit stocks (Table 2) used to calculate the estimated flux. Bank water, solids and TOC were the largest fluxes and similar in magnitude at −2762 ± 403, −2106 ± 262, 153 ± 24 Gg yr^{-1} over the longer term, followed by Ca, TN, Mg, Na, and K at −10687 ± 1509, −7762 ± 1324, −1100 ± 144, −724 ± 123, −722 ± 123, and −156 ± 25 Gg yr^{-1}. These fluxes represent minimum estimates because they do not include material stores below the sea level, which could also be exported to the ocean during coastal erosion.

4. Discussion

4.1. Carbon and Other Material Stores

[26] The range of soil stores we found along the Arctic coast was comparable to that found for northern Alaska and Canada by *Ping et al.* [2008] and *Jorgenson and Brown* [2005], Our sampling was deeper than most studies and revealed that dislocated and buried peat from cryoturbation

Table 3. Effects of Coastal Type and Geomorphic Unit on Soil Properties Based on One-Way Analysis of Variance[a]

Soil Property	Coastal Type		Geomorphic Unit	
	F	*P* Value	F	*P* Value
Erosion rate (long term)	1.09	0.37	10.86	0.00
Erosion rate (recent)	1.49	0.22	15.17	0.00
Bank height	7.87	0.00	7.47	0.00
Wedge ice	3.10	0.03	24.67	0.00
Solids	1.91	0.13	16.37	0.00
H_2O	8.04	0.00	4.70	0.00
TOC	4.86	0.00	4.18	0.00
TN	6.82	0.00	3.36	0.01
Ca	2.16	0.09	8.84	0.00
Mg	3.42	0.02	2.34	0.04
K	1.69	0.17	1.59	0.17
Na	0.27	0.90	2.92	0.02

[a]Abbreviations are as follows: TN, total nitrogen; TOC, total organic carbon.

can be found considerably deeper than commonly thought; organic samples were frequently obtained from 1 to 2 m depths and occasionally from 2 to 3 m depths. Moreover, in previous studies [*Bockheim et al.*, 2004] soil organic matter at 80–160 cm depths stored in drained-lake basins was treated as depositional from thaw lake events. Our study indicates that organic matter can be dislocated and moved deeper through freeze-thaw processes and syngenetic permafrost development under many geomorphic environments and merits further study.

[27] Ground ice is abundant in most permafrost soils, but is often overlooked in estimates of soil carbon and material fluxes. In our study we fully accounted for the volumetric contents of both segregated and wedge ice. Wedge ice alone can offset up to 30% of the C and N stores, and wedge plus segregated ice occupy 70 to 80% of the total volume of soil in the permafrost-affected Arctic Coastal Plain. This ground ice contributes to the export of a large amount of water, although this amount is minuscule in terms of its contribution to sea level rise. On the terrestrial side, the ground ice is critical to the response of coastal zone to climate warming and permafrost degradation because it reduces the elevation of the ground surface, thus allowing the land to be more susceptible to flooding from storm surges. This is most dramatic in the Cape Halkett area where large thaw-lake basins extend tens of kilometers inland and have extensive salt-killed shoreline vegetation.

[28] The geomorphic classification was effective at partitioning the variability in soil carbon, nitrogen and materials stores, and ground ice contents because it relates soil materials with erosional and depositional processes that occur over varying time periods. The highest carbon stores were found in sandy diamicton and glaciomarine deposits, which are the oldest deposits being of late Pleistocene age. Thus they have been accumulating OC and N for most of the Holocene. In contrast, ice-poor basins and delta deposits are the youngest deposits, being of middle to late Holocene age and have the lowest OC and N stores. The classification, which differentiated older ice-rich and younger ice-poor basins on the basis of the amount of surface polygonization, revealed large differences in water stores (ice) between the deposits. Eolian sand had intermediate water and OC stores, but results were affected by our grouping of both young active and late Pleistocene inactive dunes for the analysis. When considered separately, active eolian deposits have very low water and carbon stores. Because the geomorphic classification was effective at partitioning the variability in OC, N and ground ice contents, it will be useful in assessing the vulnerability of the coast to future erosion, thawing, and flooding. Bank height of course is important in estimation of all stores and varied fivefold among units.

4.2. Material Flux Into the Arctic Ocean

[29] Our estimates of fluxes fully accounted for soil properties (particularly frozen bulk densities), ground ice, bank heights and erosion rates, whereas, previous estimates [*Jorgenson and Brown*, 2005] had relied on very incomplete data sets extrapolated across more generalized units. Geomorphic units separated annual TOC flux estimates into a wider range (12x: 10 to 122 kg TOC m^{-1} yr^{-1}) compared to the coastal types (8x: 21 to 163 kg TOC yr^{-1}). Bank stores also had wider ranges among geomorphic units compared to coastal types. Although variability within units is high for both systems, the data indicate that geomorphic units provides a better classification for partitioning the many factors important in material fluxes including erosion rates, soil carbon, ice content, bank height, and total bank materials. Ideally a coastal classification system would incorporate elements of both systems, but we did not integrate both systems for this study because our sample sizes would have been inadequate to test for differences among the numerous classes that would be generated by combining the systems.

[30] Quantitative estimates of material fluxes are fraught with many challenges. First, the extremely high variability in wedge ice distribution and segregated ice, and the cryoturbation of organic matter through the upper profile led to high variability and wide confidence limits. This high variability reduced our ability to find significant differences among coastal types. In future studies this could be over-

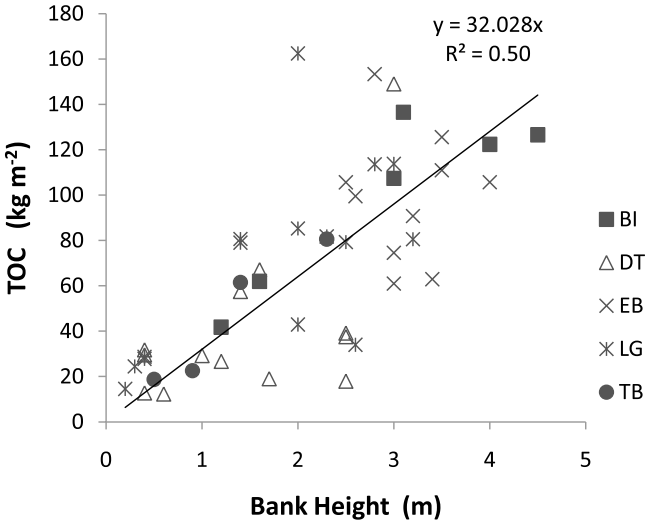

Figure 3. Soil properties most affected by coastal type and geomorphic unit. Vertical axis represents average value of the soil property, with standard deviation, under various categories of coastal type and geomorphic unit. BI, bay inlet; DT, delta; EB, exposed bluff; LG, lagoon; TB, tapped basin.

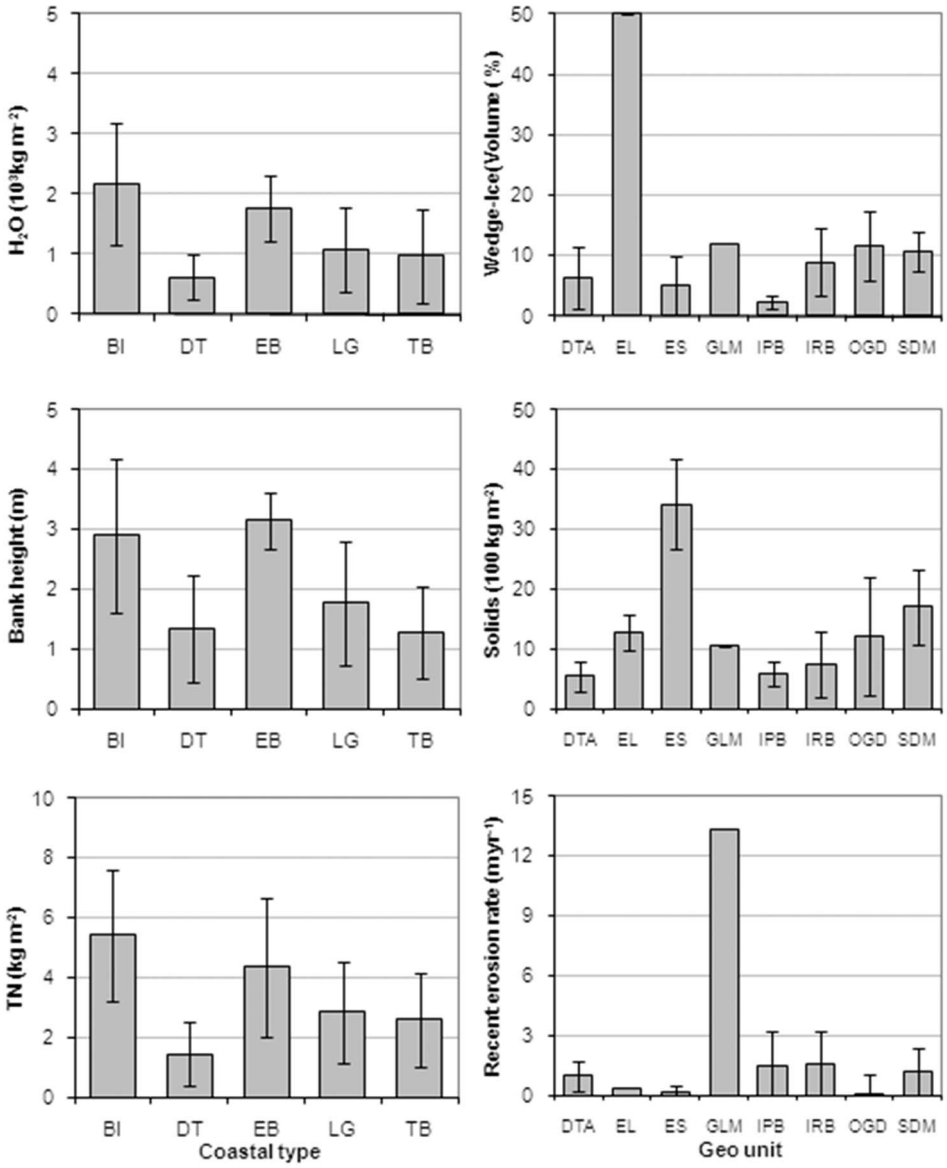

Figure 4. Site total organic carbon stores as they vary with bank height with coastal types identified by different markers. Costal types: BI, bay inlet; DT, delta; EB, exposed bluff; LG, lagoon; TB, tapped basin. Geomorphic units: DTA, delta and tidal flat; EL, eolian loess; ES, eolian sand; GLM, glaciomarine; IPB, ice-poor basin; IRB, ice-rich basin; OGD, other gravel deposits; SDM, sandy diamicton.

come by greatly increasing sample sizes, although this greatly increases the expense of such an effort. Second, we used the contemporary water line to define the base of the coastline because this was the only consistent feature for defining the shore boundary over varied geomorphic units. However, the error introduced by this methodology was relatively minor. On the basis of a tidal variation of 20 cm, departure from mean water level probably was less than 10 cm at the time of the image acquisition and field sampling. Error associated with this tidal variation was probably small (<1 m inshoreline position at most sites in relation to an average 50.6 m change over a ~50 year period). Similarly, the error from tidal variation that was incorporated into estimated material stores above water level was small (<10 cm in relation to an average bank height of 2.0 m). Georectification of imagery also contributed a small error (~3 m RMS positional error in relation to an average 50.6 m change over a ~50 year period). Overall, the contribution of these sampling errors was small (probably <5%) in relation to the problems caused by high sampling variability and consequential large confidence limits (15% of mean value) of our flux estimates.

[31] On the basis of our estimated fluxes and scaled up to pan-Arctic regions [*Rachold et al.*, 2004; *McGuire et al.*, 2009], coastal erosion contributes about 15% of the total terrigenous OC flux to the Arctic Ocean (41 Tg yr^{-1}). However, the lateral export fluxes from pan-Arctic erosion are in the same order of riverine fluxes of particulate organic

Table 4. Estimated Total Flux of Materials Along the Coastal Type Segments of the 1957 km Coastline[a]

Coastal Type Segment[b]	Time Period	Erosion Rate (m yr^{-1})	Coastal Segment Annual Flux							
			Solids (Gg yr^{-1})	Water[c] (Gg yr^{-1})	TOC (Gg yr^{-1})	TN (Mg yr^{-1})	Extractable K (Mg yr^{-1})	Extractable Ca (Mg yr^{-1})	Extractable Mg (Mg yr^{-1})	Extractable Na (Mg yr^{-1})
DT (691 km)	1950–1980	−0.2	−164	−66	−6	−184	−5	−742	−33	−24
	1980–2000	−0.6	−306	−235	−16	−652	−37	−1180	−177	−270
	1950–2000	−0.5	−309	−241	−16	−723	−20	−1371	−125	−147
LG (547 km)	1950–1980	−0.8	−399	−510	−32	−1657	−25	−2503	−264	−191
	1980–2000	−0.9	−479	−566	−36	−1519	−29	−3222	−285	−188
	1950–2000	−1.0	−543	−642	−40	−1865	−30	−3607	−315	−193
EB (313 km)	1950–1980	−1.0	−461	−590	−30	−1452	−22	−2595	−218	−121
	1980–2000	−2.5	−1064	−1420	−81	−4264	−51	−4306	−402	−157
	1950–2000	−1.8	−722	−1024	−56	−2904	−36	−3436	−315	−147
BI (235 km)	1950–1980	−1.0	−290	−490	−24	−1286	−36	−1518	−185	−122
	1980–2000	−1.2	−314	−485	−24	−1310	−32	−1571	−201	−111
	1950–2000	−1.2	−335	−550	−27	−1454	−39	−1727	−214	−133
TB (171 km)	1950–1980	−0.9	−79	−140	−7	−396	−19	−269	−72	−68
	1980–2000	−2.5	−217	−458	−21	−1216	−44	−796	−192	−145
	1950–2000	−1.6	−147	−305	−14	−815	−31	−537	−131	−104

Total Coastline (km)	Coastline Average[d]		Full Coastline Annual Flux							
	Time Period	Erosion Rate[d] (m yr^{-1})	Solids (Gg yr^{-1})	Water[c] (Gg yr^{-1})	TOC (Gg yr^{-1})	TN (Mg yr^{-1})	Extractable K (Mg yr^{-1})	Extractable Ca (Mg yr^{-1})	Extractable Mg (Mg yr^{-1})	Extractable Na (Mg yr^{-1})
1957	1950–1980	**−0.6**	**−1393**	**−1796**	**−98**	**−4975**	**−107**	**−7627**	**−722**	**−527**
	CI	*±0.5*	*±236*	*±275*	*±15*	*±761*	*±23*	*±1536*	*±134*	*±120*
	1980–2000	**−1.2**	**−2381**	**−3164**	**−178**	**−8961**	**−193**	**−11076**	**−1258**	**−870**
	CI	*±1.0*	*±429*	*±481*	*±28*	*±1476*	*±30*	*±2527*	*±177*	*±154*
	1950–2000	**−1.0**	**−2106**	**−2762**	**−153**	**−7762**	**−156**	**−10678**	**−1100**	**−724**
	CI	*±0.8*	*±262*	*±403*	*±24*	*±1324*	*±25*	*±1509*	*±144*	*±123*

[a]Separate flux estimates for sites averaged within coastal types are based on erosion rate averages within coastal types over the different time periods 1950–1980, 1980–2000, and 1950–2000 (Table 1) using the average bank height stores for sites within coastal types (Table 2). The estimated rates of coastline area loss for these time periods using the average erosion rate are 117 ± 98 ha yr^{-1} during 1950–1980, 235 ± 196 ha yr^{-1} during 1980–2000, and 203 ± 151 ha yr^{-1} during 1950–2000. Estimated total annual hectares land loss calculated using weighted average erosion rates and total coastal length of 1957 km. Abbreviations are as follows: BI, bay inlet; DT, delta; EB, exposed bluffs; LG, lagoon; TB, tapped basin. Bold values are period averages, and italic values are 95% confidence intervals.

[b]Values in parentheses are length.

[c]Includes ice wedge water.

[d]Weighted average of coastal types as they occur along the 1957 km coastline.

carbon, which is estimated at 6–7 Tg-OC yr^{-1} [*McGuire et al.*, 2009]. Actually, the riverine POC fluxes are mostly derived from the erosion of river bank and permafrost on the basis of evidence of radiocarbon composition of riverine POC and estuarine sediments [*Goni et al.*, 2005; *Guo et al.*, 2007]. In addition, while river export is restricted in the estuarine region, materials exported from coastal erosion are dispersed along the entire Arctic coastline, allowing extensive biogeochemical cycling after erosion. Lateral export fluxes of OC from coastal erosion have significant implications in Arctic carbon cycle and ecosystem changes. Although recent studies showed that only about 1–2% of the total soil OC could be released in dissolved OC form during soil leaching experiments [*Dou et al.*, 2008; *Xu et al.*, 2009a, 2009b], the inputs of soil organic matter through both coastal erosion and river export and the subsequent degradation of both dissolved and particulate organic matter may significantly alter the water and environmental quality and shift the Arctic coastal ecosystem to a net heterotrophic setting. Unfortunately, the fate of organic matter exported from coastal erosion and rivers is largely unknown [*Holmes et al.*, 2008]. Further studies are needed to examine the biogeochemical cycling of old soil organic carbon in the Arctic Ocean.

[32] In addition to export fluxes of OC and TN, coastal erosion may also contribute significantly to the export flux of major elements. Indeed, on the basis of our estimation, the annual fluxes based on longer-term erosion rates of extractable cations were 1100 ± 144 Mg for Mg, 10,678 ± 1509 Mg for Ca, 156 ± 25 Mg for K, and 724 ± 123 Mg for Na, for the 1957 km coastline (Table 4). These fluxes are 3–6% of river fluxes reported from the Mackenzie River the largest Arctic river in the North American Arctic [*Telang et al.*, 1991].

[33] There was a 100% increase in the average coastline erosion rate for the recent 1980–2000 period (−1.2 ± 1.0 m yr^{-1}) compared to the early 1950–1980 period (0.6 ± 0.5 m yr^{-1}), but the rates were highly variable among geomorphic units. For exposed bluffs, tapped basins, and delta units the average erosion rates increased about 150%, 178%, and 200%, respectively, for the recent period over the early period, while the other coastal types of bay inlets and lagoons increased only 13 and 20%, respectively (Table 4). Although the increase is substantial, the time series of imagery are insufficient to detect a long-term trend related to climate warming and sea ice retreat. Even over 20–30 year periods rates can be sensitive to a few large storm events. The increase is consistent, however, with the analyses by *Jones*

et al. [2009] for the Cape Halkett area that indicate that erosion rate are increasing in response to decreasing sea ice. Our overall rates were relatively low, however, because we incorporated the large areas of delta deposits that typically have low erosion rates and are more likely to have accreting shorelines. Deltaic erosion is low due to the low-lying flat topography that often lack distinct banks, the extensive very shallow water that limit wave height and energy, and frequent sedimentation.

5. Conclusions

[34] Stores and fluxes of soil carbon and other soil components along the eroding shoreline of the Beaufort Sea were highly variable owing to large differences in bank composition, bank heights, exposure to the open sea, and erosion rates that were found among coastal types and geomorphic units. To address the difficultly in sampling these extremely heterogeneous materials and landscapes, we used a systematic sampling approach that allowed us to produce the first flux estimates with explicit confidence limits of organic carbon, total nitrogen, major cations, and total solids along the Alaska Beaufort Sea coast. Estimates were based on detailed soil description and analysis at sites distributed across the entire 1957 km coastline. The geomorphic classification was particularly effective at partitioning a suite of important factors including erosion rates, bank heights, soil carbon, and ground ice contents. Erosion rates were extremely variable along the coast, and our long-term estimate of the average erosion rate of 1.0 ± 0.7 m yr^{-1} along the entire coast (including deltas) was less than many estimates of Arctic coastal erosion, although maximum recent (1980–2000) rates for sites along the coast were as high 13.3 m yr^{-1} along exposed portions of extremely ice-rich glaciomarine deposits. Because most coastal deposits are ice-rich they will become increasingly vulnerable to the combined effects of warming water temperatures, longer ice-free periods and increasing wave energy from reduced sea ice. Coastal erosion releases large quantities of organic carbon, as well as sediment, fresh water, nitrogen, and cations, which may affect elemental budget and biogeochemical processes in the coastal zones of the Arctic Ocean.

[35] **Acknowledgments.** This research was supported in part by the National Science Foundation Arctic System Science Program, ARC-0436179 and ARC-0436165, the USDA Hatch Project, and the Alaska EPSCoR program funded by the NSF grant 0701898 and the State of Alaska. Logistic support was provided through Barrow Scientific Consortium and VECO Polar Resources. Special thanks to Laurie Wilson at the UAF Palmer Research Center Lab for performing all soil analyses and Dorte Dissing for performing the coastal erosion photogrammetry; James and Teena at the Helmeriks Lodge for their kindness and support during the field season; and the Associate Editor and two anonymous reviewers for constructive comments.

References

Black, R. F. (1964), Gubik formation of Quaternary age in northern Alaska, *U.S. Geol. Surv. Prof. Pap.*, *302-C*, 59–91.

Bockheim, J. G., K. M. Hinkel, W. R. Eisner, and X. Y. Dai (2004), Carbon pools and accumulation rates in an age series of soils in drained thaw lake basins, arctic Alaska, *Soil Sci. Soc. Am. J.*, *68*, 697–704, doi:10.2136/sssaj2004.0697.

Brown, J., and S. Solomon (2000), Arctic coastal dynamics: Report of an international workshop, *Open File Rep. 3929*, Geol. Surv. of Can., Ottawa, Ont.

Carter, L. D. (1981), A Pleistocene sand sea on the Alaskan Arctic Coastal Plain, *Science*, *211*, 381–383, doi:10.1126/science.211.4480.381.

Dallimore, S. R., S. Wolfe, and S. M. Solomon (1996), Influence of ground ice and permafrost on coastal evolution, Richards Island, Beaufort Sea Coast, NWT, *Can. J. Earth Sci.*, *33*, 664–675.

Davidson, E. A., and I. A. Janssens (2006), Temperature sensitivity of soil carbon decomposition and feedbacks to climate change, *Nature*, *440*, 165–173, doi:10.1038/nature04514.

Dinter, D. A., L. D. Carter, and J. K. Brigham-Grette (1990), Late Cenozoic geologic evolution of the Alaskan North Slope and adjacent continental shelves, in *The Geology of the Arctic Ocean Region*, edited by A. Grantz et al., pp. 459–490, Geol. Soc. of Am., Boulder, Colo.

Dou, F., C.-L. Ping, L. Guo, and T. Jorgeson (2008), Estimating the impact of seawater on the production of soil water-extractable organic carbon during coastal erosion, *J. Environ. Qual.*, *37*, 2368–2374, doi:10.2134/jeq2007.0403.

Gibson, J. A. E., W. F. Vincent, B. Nieke, and R. Pienitz (2000), Control of biological exposure to UV radiation in the Arctic Ocean: Comparison of the roles of ozone and riverine dissolved organic matter, *Arctic*, *53*, 372–382.

Gilmanov, T. G., and W. C. Oechel (1995), New estimates of organic matter reserves and net primary productivity of the North American tundra ecosystems, *J. Biogeogr.*, *22*, 723–741, doi:10.2307/2845975.

Goni, M. A., M. B. Yunker, R. W. Macdonald, and T. I. Eglinton (2005), The supply and preservation of ancient and modern components of organic carbon in the Canadian Beaufort Shelf of the Arctic Ocean, *Mar. Chem.*, *93*, 53–73, doi:10.1016/j.marchem.2004.08.001.

Guo, L., C.-L. Ping, and R. W. Macdonald (2007), Mobilization pathways of organic carbon from permafrost to arctic rivers in a changing climate, *Geophys. Res. Lett.*, *34*, L13603, doi:10.1029/2007GL030689.

Guo, L., Y. Cai, C. Belzile, and R. W. Macdonald (2011), Sources and export fluxes of inorganic and organic carbon and nutrient species from the seasonally ice-covered Yukon River, *Biogeochemistry*, doi:10.1007/s10533-010-9545-z, in press.

Harper, J. R. (1978), Coastal erosion rates along the Chukchi Sea coast near Barrow, Alaska, *Arctic*, *31*, 428–433.

Hartwell, A. D. (1973), Classification and relief characteristics of northern Alaska's coastal zone, *Arctic*, *26*, 244–252.

Holmes, R. M., J. W. McClelland, P. A. Raymond, B. B. Frazer, B. J. Peterson, and M. Stieglitz (2008), Lability of DOC transported by Alaskan rivers to the Arctic Ocean, *Geophys. Res. Lett.*, *35*, L03402, doi:10.1029/2007GL032837.

Jones, B. M., C. D. Arp, M. T. Jorgenson, K. M. Hinkel, J. A. Schmutz, and P. L. Flint (2009), Increase in the rate and uniformity of coastline erosion in Arctic Alaska, *Geophys. Res. Lett.*, *36*, L03503, doi:10.1029/2008GL036205.

Jorgenson, M. T., and J. Brown (2005), Classification of the Alaskan Beaufort Sea coast and estimation of carbon and sediment inputs from coastal erosion, *Geo Mar. Lett.*, *25*, 69–80, doi:10.1007/s00367-004-0188-8.

Jorgenson, M. T., and Y. Shur (2008), Glaciation of the Coastal Plain of northern Alaska, *Eos Trans. AGU*, *89*(53), Fall Meet. Suppl., Abstract C11D-0544.

Jorgenson, M. T., Y. L. Shur, and E. R. Pullman (2006), Abrupt increase in permafrost degradation in Arctic Alaska, *Geophys. Res. Lett.*, *33*, L02503, doi:10.1029/2005GL024960.

Kreig, R. A., and R. D. Reger (1982), Air-photo analysis and summary of landform soil properties along the route of the Trans-Alaska Pipeline System, *Geol. Rep. 66*, 149 pp., Alaska Div. of Geol. and Geophys. Surv., Fairbanks.

Leffingwell, E. K. (1919), *The Canning River Region, Northern Alaska*, *U.S. Geol. Surv. Prof. Pap.*, 109, 249 pp.

McGuire, A. D., L. Anderson, T. R. Christensen, S. Dallimore, L. D. Guo, D. Hayes, M. Heimann, R. Macdonald, and N. Roulet (2009), Sensitivity of the carbon cycle in the Arctic to climate change, *Ecol. Monogr.*, *79*, 523–555, doi:10.1890/08-2025.1.

Michaelson, G. J., C.-L. Ping, and J. M. Kimble (1996), Carbon storage and distribution in tundra soils of Arctic, Alaska, U.S.A, *Arct. Alp. Res.*, *28*, 414–424, doi:10.2307/1551852.

Ping, C.-L., G. J. Michaelson, W. M. Loya, R. J. Candler, and R. L. Malcolm (1997), Characteristics of soil organic matter in Arctic ecosystems of Alaska, in *Soil Processes and the Carbon Cycle*, edited by R. Lal et al., pp. 157–167, CRC Press, Boca Raton, Fla.

Ping, C.-L., G. J. Michaelson, M. T. Jorgenson, J. M. Kimble, H. Epstein, V. E. Romanovsky, and D. A. Walker (2008), High stocks of soil organic carbon in North American Arctic region, *Nat. Geosci.*, *1*, 615–619, doi:10.1038/ngeo284.

Pullman, E. R., M. T. Jorgenson, and Y. Shur (2007), Thaw settlement in soils of the Arctic Coastal Plain, Alaska, *Arct. Antarct. Alp. Res.*, *39*, 468–476, doi:10.1657/1523-0430(05-045)[PULLMAN]2.0.CO;2.

Rachold, V., H. Eicken, V. V. Gordeev, M. N. Grigoriev, H.-W. Hubberten, A. P. Lisitzin, V. P. Shevchenko, and L. Schirrmeister (2004), Modern terrigenous organic carbon input to the Arctic Ocean, in *The Organic Carbon Cycle in the Arctic Ocean*, edited by R. Stein and R. W. Macdonald, pp. 33–54, Springer, Berlin.

Raymond, P. A., J. W. McClelland, R. M. Holmes, A. V. Zhulidov, K. Mull, B. J. Peterson, R. G. Striegl, G. R. Aiken, and T. Y. Gurtovaya (2007), Flux and age of dissolved organic carbon exported to the Arctic Ocean: A carbon isotopic study of the five largest arctic rivers, *Global Biogeochem. Cycles*, *21*, GB4011, doi:10.1029/2007GB002934.

Savelieva, N. I., I. P. Semiletov, L. N. Vasilevskaya, and S. P. Pugach (2000), A climate shift in seasonal values of meteorological and hydrological parameters for northeastern Asia, *Prog. Oceanogr.*, *47*, 279–297, doi:10.1016/S0079-6611(00)00039-2.

Shur, Y. L., and M. T. Jorgenson (1998), Cryostructure development on the floodplain of the Colville River Delta, northern Alaska, in *Proceedings of the Seventh International Conference on Permafrost*, edited by A. G. Lewkowicz and M. Allard, *Collect. Nordicana*, 57, 993–1000.

Soil Survey Laboratory Staff (1996), Soil survey laboratory methods manual, *Soil Surv. Invest. Rep. 42*, Natl. Soil Surv. Cent., U.S. Dep. of Agric. Nat. Resour. Conserv. Serv., Lincoln, Nebr.

Stein, R., and R. W. Macdonald (2004), Organic carbon budget: Arctic Ocean vs. global ocean, in *The Organic Carbon Cycle in the Arctic Ocean*, edited by R. Stein and R. W. Macdonald, pp. 315–322, Springer, New York.

Telang, S. A., R. Pocklington, A. S. Naidu, E. A. Romankevich, I. I. Gitelson, and M. I. Gladyshev (1991), Carbon and mineral transport in major North American, Russian Arctic, and Siberian rivers: The St. Lawrence, the Mackenzie, the Yukon, the Arctic Alaskan rivers, the Arctic Basin rivers in the Soviet Union, and the Yenisei, in *Biogeochemistry of Major World Rivers*, edited by E. T. Degens, S. Kempe, and J. E. Richey, *SCOPE*, 42, 75–104.

Thieler, R. E., E. A. Himmelstoss, J. L. Zichichi, and T. L. Miller (2005), User guide and tutorial for the digital shoreline analysis system, *U.S. Geol. Surv. Open File Rep.*, *2005-1304*, 1–33.

Wahrhaftig, C. (1965), Physiographic divisions of Alaska, *U.S. Geol. Surv. Prof. Pap.*, *482*, 1–52.

Walker, H. J. (1983), Erosion in a permafrost-dominated delta, in *Permafrost: Fourth International Conference Proceedings*, pp. 1344–1349, Natl. Acad. Press, Washington, D. C.

Xu, C. H., L. D. Guo, F. Dou, and C.-L. Ping (2009a), Potential DOC production from size fractionated Arctic tundra soils, Alaska, *Cold Reg. Sci. Technol.*, *55*, 141–150, doi:10.1016/j.coldregions.2008.08.001.

Xu, C. H., L. D. Guo, C.-L. Ping, and D. M. White (2009b), Chemical and isotopic characterization of size-fractionated organic matter from cryoturbated tundra soils, northern Alaska, *J. Geophys. Res.*, *114*, G03002, doi:10.1029/2008JG000846.

F. Dou, Texas AgriLife Research and Extension Center, Texas A&M University, 1509 Aggie Dr., Beaumont, TX 77713, USA.

L. Guo, Department of Marine Science, University of Southern Mississippi, Stennis Space Center, MS 39529, USA.

M. T. Jorgenson, ABR Inc., Fairbanks, AK 99708, USA.

M. Kanevskiy and Y. Shur, Department of Civil and Environmental Engineering, University of Alaska Fairbanks, Fairbanks, AK 99775, USA.

J. Liang, Department of Forest Sciences, School of Natural Resources and Agricultural Sciences, University of Alaska Fairbanks, Fairbanks, AK 99775, USA.

G. J. Michaelson and C.-L. Ping, Palmer Research Center, School of Natural Resources and Agricultural Sciences, 533 E. Fireweed Ave., University of Alaska Fairbanks, Palmer, AK 99645, USA. (cping@alaska.edu)